

67 SAN098-0880C

GRADIENT-DRIVEN DIFFUSION USING DUAL CONTROL VOLUME GRAND
CANONICAL MOLECULAR DYNAMICS*

(Draft) SAND-98-0880C
RECEIVED
CONF-980604-APR 23 1998

Aidan M. Thompson[‡], David M. Ford[†], and Grant S. Heffelfinger[‡]

OSTI

[‡]Materials Simulation Science Department, Sandia National Laboratories, P.O. Box 5800, Albuquerque, NM 87185-1111, USA and [†]Department of Chemical Engineering, Texas A&M University, College Station, TX 778943-3122, USA

The dual control volume grand canonical molecular dynamics (DCV-GCMD) method, designed to enable the dynamic simulation of a system with a steady-state chemical potential gradient is first briefly reviewed. A new, novel implementation of the method which enables the establishment of a steady state chemical potential gradient in a multicomponent system without having to insert or delete one of the components is then presented and discussed.

1. INTRODUCTION

The basis for the DCV-GCMD method¹ is the idea that if two local “grand canonical Monte Carlo control volumes” are placed inside the simulation volume of a molecular dynamics simulation and grand canonical Monte Carlo (GCMC) insertions and deletions are carried out to establish different desired chemical potentials in these control volumes, equilibration exchanges between the MD simulation volume and the GCMC control volumes will establish a steady-state chemical potential gradient between the control volumes.

GCMD methods which employ two local chemical potential control volumes (i.e. “dual control volume” GCMD) have been applied to bulk diffusion, diffusion and flow in confined fluids, and diffusion of gases in polymers. Other recent work has included the development of massively parallel versions of DCV-GCMD for both atomic⁴ and molecular⁵ systems.

DTIC QUALITY INSPECTED 2

*This work was performed at Sandia National Laboratories which is operated for the DOE under contract number DE-AC04-94AL85000.

DISCLAIMER

This report was prepared as an account of work sponsored by an agency of the United States Government. Neither the United States Government nor any agency thereof, nor any of their employees, makes any warranty, express or implied, or assumes any legal liability or responsibility for the accuracy, completeness, or usefulness of any information, apparatus, product, or process disclosed, or represents that its use would not infringe privately owned rights. Reference herein to any specific commercial product, process, or service by trade name, trademark, manufacturer, or otherwise does not necessarily constitute or imply its endorsement, recommendation, or favoring by the United States Government or any agency thereof. The views and opinions of authors expressed herein do not necessarily state or reflect those of the United States Government or any agency thereof.

2. SIMULATION METHODS

DCV-GCMD can be thought of as a hybridization of MD and GCMC: each atom in the system is moved with the normal MD algorithm during an “MD phase”. Each MD phase is followed by a “GCMC phase” in which creations, destructions, and (if desired) identity swaps of each component are attempted in each GCMC control volume. Destroyed atoms are simply removed from the simulation while created atoms are assigned velocities chosen on a Gaussian distribution. After the GCMC phase, the simulation proceeds with another MD timestep, and so on. The method and companion parallel algorithms have been discussed elsewhere^{1,4,5}.

Periodic boundary conditions are applied in the dimensions appropriate for the simulated system. The density profile, $\rho_i(x)$, is calculated by dividing the system volume into bins along the x -axis and averaging the number of atoms of type i in each bin. The flux between the two control volumes can be measured in three different ways. In the planar flux method (Figure 1), the net movement of each species type, i , across a stationary plane is used to calculate the flux. In the control volume method, the net number of particles added or subtracted in each control volumes is used to determine the flux. In a third method, flux profiles are calculated using a binning system (analogous to that used for the density profiles) for the x -velocities of the atoms of each type, enabling the flux of component i to be calculated as a function of x -position.

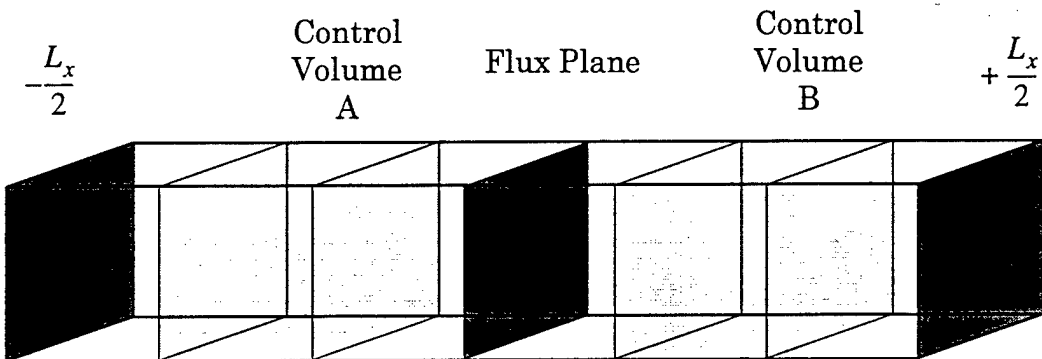


Figure 1. A schematic of a DCV-GCMD simulation. Two control volumes, A and B, are used for creations/destinations to achieve spatial chemical potential control of each species in the system. The flux planes are shown as the dark shaded planes between the control volumes and at the x -direction periodic boundaries, $x = \pm L_x/2$.

2.1. Chemical Potential Control for Large Molecules

Until recently the DCV-GCMD method has not been applicable to systems with molecules which are too large to be inserted and deleted. Our approach, originally due

19980507
066

to Van Swol and Heffelfinger², is to circumvent the problem of insertion/deletion altogether by the exchange of one field variable, in this case μ_n , the chemical potential of the n th component, for total pressure, P . This is accomplished by carrying out insertions and deletions on the other species in the system, $i = 1, n-1$, to establish constant chemical potential for those species, $\mu_{i=1,n-1}$, while keeping the system pressure constant. This enables the establishment of constant chemical potential for species n , the large molecular species, for the price of a fixed number of atoms of that species, N_n .

The system pressure is controlled by introducing a pair of moving walls (pistons) at either end of the simulation box following the method introduced by Lupkowski and van Swol⁶. The pistons, free to move in the x -direction, interact with the fluid atoms via a short-ranged repulsive potential. The repulsive force of the fluid on the pistons is counteracted by a constant restraining force which is set equal to the desired system pressure. Each piston is assigned a mass, and its motion in the x -direction is treated as if it were another particle. As a result, once the system has equilibrated, the force exerted by the atoms on the piston will fluctuate about that of the constant restraining force thus maintaining a constant average pressure in the x -direction in the fluid near the wall. Implicit in this approach is the assumption that the same pressure is imposed on both pistons, i.e. there is no pressure gradient in the system.

3. Applications of the DCV-GCMD Method

The DCV-GCMD method has been applied to a variety of systems with the Lennard-Jones model for site-site interactions. The original work on the DCV-GCMD method¹ was designed to check the validity of the method for determining diffusivities in the presence of a chemical potential gradient. In order to enable comparison to equilibrium diffusivities obtained from a standard NVT molecular dynamics simulation, a color diffusion “experiment” was carried out: two components, with identical interaction parameters, were simply “labeled” as species 1 and species 2. Equal and opposite chemical potential gradients were established and the flux and steady state density profiles used to calculate the diffusivities of each in the presence of a chemical potential gradient of *that species*. However, for the system as a whole (labeling aside), no chemical potential gradient existed. The diffusivities calculated from the fluxes

and density profiles were found to match those of the corresponding standard *NVT* MD simulation¹.

The DCV-GCMD method has also been used to investigate “uphill diffusion” in a bulk ternary Lennard-Jones system². In order to create nonideal conditions sufficient to establish the steady-state uphill diffusion phenomena, the Lennard-Jones cross-parameters were varied until nonideality sufficient to induce the uphill diffusion effect was obtained.

Another application of DCV-GCMD has been to bonded systems⁵. This system consisted of the two single-site species, 1 and 2, with identical interaction parameters, plus a polymer component, species 3. The polymer was modeled as a set of linear chains with 50 interaction sites (beads) each, with neighboring beads linked by FENE bonds. All beads and species 1 and 2 molecules had an identical mass and Lennard-Jones interaction parameters. Only species 1 and 2 were inserted and deleted and two polymer bead densities were investigated, $\rho\sigma^3 = 0.25$ and $\rho\sigma^3 = 0.85$.

3.1. Constant Pressure DCV-GCMD

In order to test the performance of the pistons in the context of gradient-driven diffusion, we applied the modified DCV-GCMD method to the binary system previously modeled by Heffelfinger and Van Swol¹ and discussed briefly above. In the first comparison, a constant-volume system was simulated using a standard DCV-GCMD simulation (constant μ_1 , μ_2 , T , V). The temperature and chemical potentials in the control volumes for both species were the same as those used by Heffelfinger and van Swol. The control volume concentrations, density profiles, and overall density agreed closely. The corresponding diffusion coefficients, calculated by assuming that $D_i^x = -J_i^x/(d\rho_i/dx)$ and using the methodology of Heffelfinger and Van Swol also agreed closely. The final flux profiles had two interesting features. Firstly, within each gradient zone, the flux profiles were uniform. However, for a given gradient zone, the fluxes of the two components did not balance, nor did the fluxes of a given component of equal and opposite size in the two gradient zones. The values of the relative flux $J_1^x - J_2^x$ in the two gradient zones were almost exactly equal and opposite. Secondly, within the control volumes, all three flux profiles were relatively noisy, but varied continuously from the value of the flux in one gradient zone, through zero, to the value of the flux in the other gradient zone. Ideally (in the limit of an infinite number of GCMC cycles per MD timestep), the relative flux within each control volume

would be zero, and there would be a discontinuity at each control volume boundary. The same would be true of the concentration gradients. In practice, both the concentration gradients and the fluxes change rapidly near the boundaries, and are relatively flat in the center of the control volumes.

Having established a benchmark using constant-volume DCV-GCMD, we then simulated the same system at constant pressure using piston pressure control instead of inserting and deleting component 2 (constant μ_1, N_2, T, P). This constant-pressure simulation was started from an empty box with fixed pistons located at $\pm 36\sigma$ and using insertions and deletions of both species to develop an equilibrated system. From this configuration, the constant-pressure simulation was executed for 300,000 timesteps. The pressure was set at $1.4\sigma^3/\epsilon$ (equal to the average pressure from the constant-volume simulation). While the number of atoms of component 1 was allowed to vary through insertions and deletions in the control volumes to achieve the desired chemical potential of component 1 in control volumes A and B, the number of atoms of component 2 remained fixed.

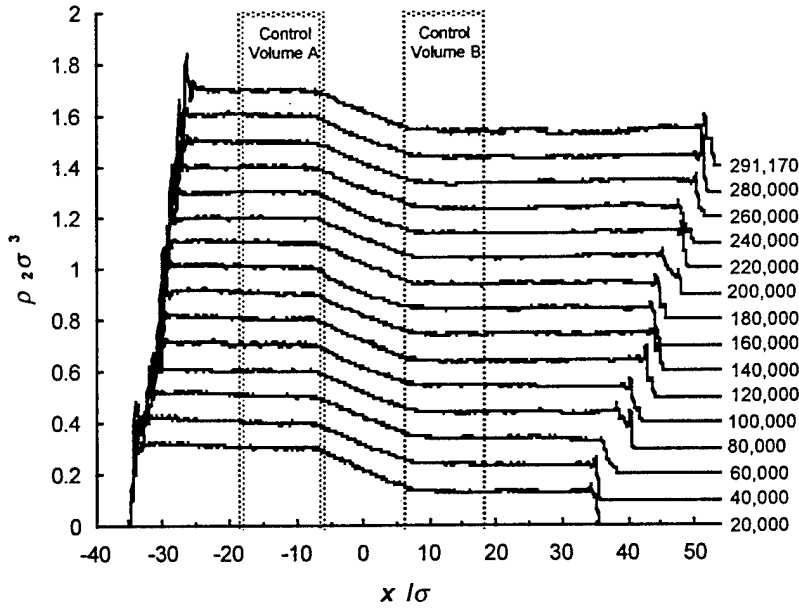


Figure 2. Time evolution of the concentration profile for component 2 in the constant-pressure DCV-GCMD simulation. Each line represents the average concentration profile accumulated over 20,000 timesteps; plot labels indicate the last timestep sampled. For clarity all the lines except the lowest have been offset vertically by successive increments of $\rho\sigma^3 = 0.1$. The grey lines represent the boundaries of the control volumes.

The evolution of the concentration profile during consecutive 20,000 timestep intervals for component 2 is contained in Figure 2. In this figure we can see how the left buffer shrinks, the right expands, and the central portion of the simulation box does not change. The right buffer actually grows faster than the left buffer shrinks because the density of component 2 is lower on the right. The simulation actually terminated when the right piston position exceeded 54σ .

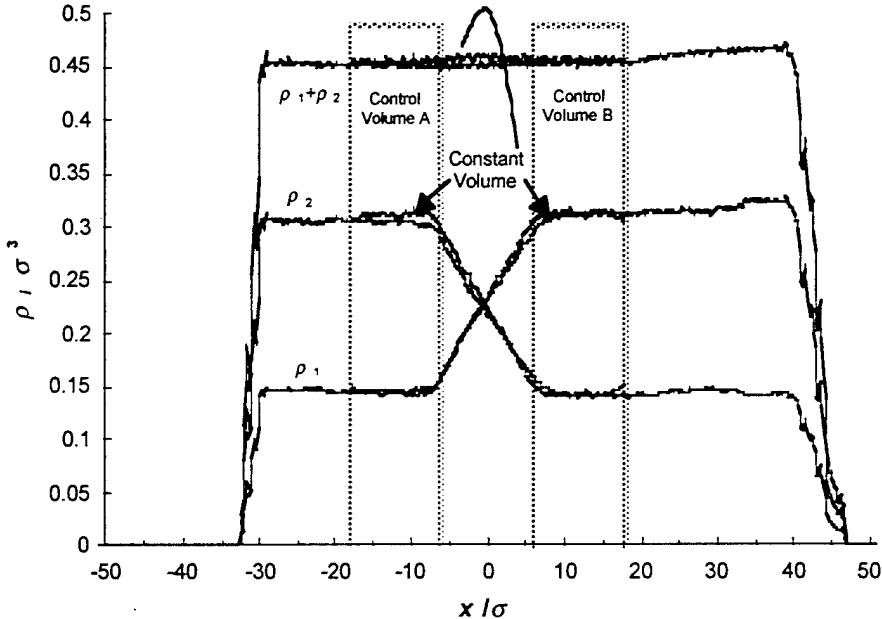


Figure 3. Average concentration profiles sampled between timesteps 100,000 and 200,000 of the constant-pressure DCV-GCMD simulation. The thicker lines are the profiles from the central region of the constant-volume DCV-GCMD simulation. The grey lines represent the boundaries of the control volumes.

The density and flux profiles sampled between timesteps 100,000 and 200,000 of the simulation are shown in Figure 3 and Figure 4. The central portions of the concentration profiles from the constant-volume simulation have been included for comparison. The agreement was close, but the constant-pressure simulations suffered a little more from “bleeding” at the control volume boundary, and consequently exhibited a slightly smaller concentration gradient. Also, the constant-pressure concentration profile within the gradient zone is not as perfectly linear as that for the constant-volume simulation.

The component flux profiles differ dramatically from those obtained by the corresponding constant-volume simulation. In the buffer zones, both components are flowing in the positive x -direction. This behavior is due to the bulk motion of the pistons

from left to right. In the gradient zone, component 1 is diffusing strongly, in the negative x -direction, while the flux of component 1 is roughly constant throughout the box.

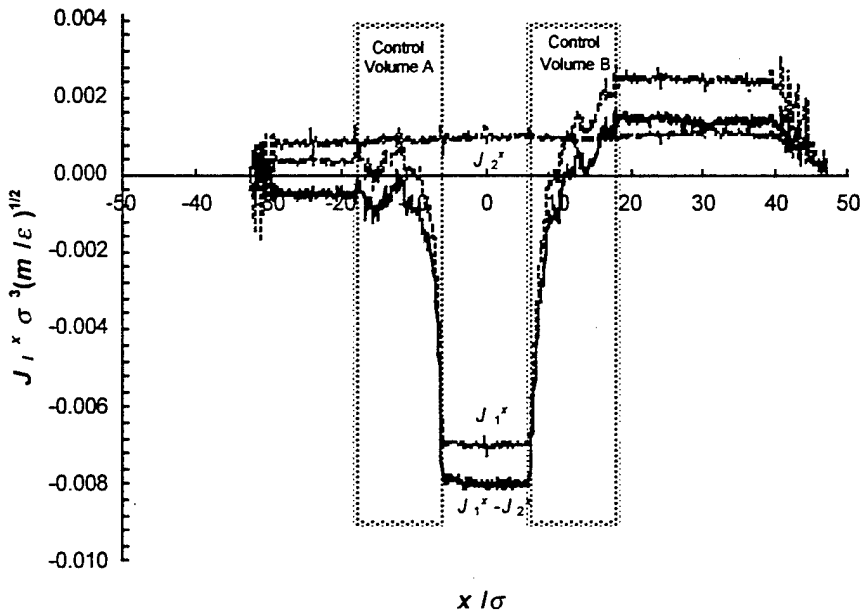


Figure 4. Average flux profiles sampled between timesteps 100,000 and 200,000 of the constant-pressure DCV-GCMD simulation. The dashed lines are the individual component fluxes, measured relative to the “stationary coordinate reference frame”, i.e. the simulation box coordinates. The solid line is the flux of component 1 relative to component 2 and is an approximation to the true molar diffusion flux. The grey lines represent the boundaries of the control volumes.

The question remains as to how the diffusion coefficient can be calculated from the constant-pressure simulation. Clearly, defining $D_i^x = -J_i^x/(d\rho_i/dx)$ no longer makes sense, as the system is now undergoing bulk motion. In this case, the molar flux J_i^x must be replaced by the more general molar diffusive flux J_{iD}^x , which is given by⁷

$$J_{iD}^x = J_i^x - x_i(J_1^x + J_2^x) \quad (1)$$

where x_i is the mole fraction of component i . In general, it is necessary to evaluate J_{iD}^x , $d\rho_i/dx$ and D_i^x as a function of position, and this analysis is carried out elsewhere⁸. For now, we have simplified the analysis by invoking the following approximation, which is exact only at the point where the concentration profiles cross each other:

$$\begin{aligned} J_{1D}^x &= (1/2)(J_1^x - J_2^x) - (1/2)(x_1 - x_2)(J_1^x + J_2^x) \\ &\approx (1/2)(J_1^x - J_2^x) \end{aligned} \quad (2)$$

As can be seen from Figure 4, $|J_1^x - J_2^x|$ is relatively invariant throughout the gradient zone, having an average value of $|J_1^x - J_2^x| \sigma^3 (m/\varepsilon)^{1/2} = 0.0080$. In the case of the constant-volume simulation, $|J_1^x - J_2^x| \sigma^3 (m/\varepsilon)^{1/2}$ was 0.0077 in the central gradient zone and 0.0080 in the periodic gradient zone, giving an average value of 0.0079. The diffusion coefficients calculated using these fluxes are given in Table . While the diffusion fluxes from both simulations are very close, the concentration gradients from the constant-pressure simulation are lower, resulting in a somewhat higher estimate of the diffusion coefficient.

Table 1: Concentration gradients, molar diffusion fluxes and transport diffusion coefficients from the constant-volume and constant pressure simulations.

Species	Constant Volume DCV-GCMD			Constant Pressure DCV-GCMD		
	$\sigma^4 d\rho_i/dx$	$J_{iD}^x \sigma^3 (m/\varepsilon)^{1/2}$	$D_i^x (m/\varepsilon)^{1/2}/\sigma$	$\sigma^4 d\rho_i/dx$	$J_{iD}^x \sigma^3 (m/\varepsilon)^{1/2}$	$D_i^x (m/\varepsilon)^{1/2}/\sigma$
1	0.0124	0.00394	0.317	0.0106	0.00399	0.376
2	0.0122	0.00394	0.323	0.0109	0.00399	0.366
Ave.	0.0123	0.00394	0.320	0.0108	0.00399	0.371

4. Conclusions

we may have some space here for some brief conclusions ...

5. REFERENCES

- 1) G. S. Heffelfinger and F. van Swol, *J. Chem. Phys.*, **100**, 7548 (1994).
- 2) F. van Swol and G. S. Heffelfinger, *Mat. Res. Soc. Symp. Proc.*, **408**, 299 (1996).
- 3) J. M. D. MacElroy, *J. Chem. Phys.*, **101**, 5274 (1994).
- 4) G. S. Heffelfinger and D. M. Ford, accepted, *Mol. Phys.* (1997).
- 5) D. M. Ford and G. S. Heffelfinger, accepted, *Mol. Phys.* (1997).
- 6) M. Lupkowski and F. van Swol, *J. Chem. Phys.*, **93**, 737 (1990).
- 7) R. Taylor, and R. Krishna, *Multicomponent Mass Transfer*, (Wiley, 1993).
- 8) A. P. Thompson and G. S. Heffelfinger, in progress.

M98004677



Report Number (14) SAND-98-0880C
CONF-980604--

Publ. Date (11)

1998-06-14

Sponsor Code (18)

DOE/CR, XF

UC Category (19)

UC-900, DOE/ER

DOE